Electrical Tuning of the Excitonic Insulator Ground State of Ta_2NiSe_5

Keisuke Fukutani [1,*] Roland Stania,[1] Jiwon Jung,[1,2] Eike F. Schwier,[3] Kenya Shimada,[3]
Chang Il Kwon,[1,2] Jun Sung Kim,[1,2] and Han Woong Yeom[1,2,†]

[1]*Center for Artificial Low Dimensional Electronic Systems, Institute for Basic Science (IBS), Pohang 37673, Republic of Korea*
[2]*Department of Physics, Pohang University of Science and Technology (POSTECH), Pohang 37673, Republic of Korea*
[3]*Hiroshima Synchrotron Radiation Center, Hiroshima University, 2-313 Kagamiyama, Higashi-Hiroshima, Hiroshima, Japan*

We demonstrate that the excitonic insulator ground state of Ta_2NiSe_5 can be electrically controlled by electropositive surface adsorbates. Our studies utilizing angle-resolved photoemission spectroscopy reveal intriguing wave-vector-dependent deformations of the characteristic flattop valence band of this material upon potassium adsorption. The observed band deformation indicates a reduction of the single-particle band gap due to the Stark effect near the surface. The present study provides the foundation for the electrical tuning of the many-body quantum states in excitonic insulators.

Introduction.—Understanding exotic ground states of matter induced by various types of many-body interactions, such as superconductivity and a charge density wave, as well as manipulating unique properties of such states, have been among the central challenges in condensed matter physics, both for the purposes of fundamental interest as well as technological advancements. Among such exotic ground states formed by many-body interactions, one finds the excitonic insulator (EI), the spontaneous condensation of excitons in narrow-gap semiconductors or semimetals at finite temperatures, stabilized by the Coulomb interaction between electrons and holes. In recent years, the EI has attracted a great deal of attention due to the growing evidence of its experimental realization [1–6], more than half a century after its theoretical predictions [7–9].

In particular, Ta_2NiSe_5 (TNS) is considered as an ideal material to investigate the nature of an EI phase, as it possesses a direct band gap at the Γ point and does not exhibit any charge density wave transition [10]. TNS has been extensively studied in the last few years and various evidence for its EI phase at low temperature have been presented. Experimental evidence includes angle-resolved photoemission spectroscopy (ARPES) studies showing the characteristic flattening of the valence band top with the formation of a band gap [4–6,11–14], infrared and optical spectroscopy studies showing the optical gap, the giant Fano resonance [15], exciton-phonon coupling [16,17] and the coherence in the order parameter [18], transport studies on bulk and thin-film samples [19], as well as scanning tunneling spectroscopy revealing a strong interband interaction [20].

Furthermore, there have been several studies devoted to tuning the EI phase. Transport studies indicated that chalcogen substitutions in TNS increase the single-particle (normal phase) band gap, lowering the EI transition temperature [21]. Laser-based ARPES [22] showed the

light-induced transient band gap narrowing [23]. Since the underlying interaction of an EI ground state is the Coulomb attraction, it is also natural to expect the susceptibility to changes in electrostatic environments, such as the free carrier screening and the applied electric field. The latter is particularly important as there has been considerable research devoted to studying heterostructure-based excitonic insulators under magnetic and electric fields [24–28], which revealed the signatures of excitonic superfluidity [24], quantum Hall phases [25,26], and the possible existence of topological excitonic insulator [27,28]. Thus, identifying and understanding the possible electrical tunability of the EI phase and corresponding band structures underlay an essential foundation for exploiting their unique properties in future device applications.

In this study, we employed high-resolution ARPES to investigate how the EI ground state of TNS is modified by the static charge doping from potassium (K) adsorbates on the surface. Our results show that the K adsorption on TNS results in the deformation of the flattened valence band top, producing evidence of the wave-vector(k)-dependent enhancement of the excitonic gap. The results are well explained by the reduction of the single-particle band gap, expected from the dipole-layer-induced Stark effect on valence and conduction bands, while the contribution from the carrier screening is found to be negligible. The present study thus successfully demonstrates the electrostatic tuning of an excitonic insulator.

Experiments.—Single crystals of TNS were grown by the chemical vapor transport method with iodine as a transport agent, and their crystallinity and stoichiometry were confirmed by x-ray diffraction and energy-dispersive spectroscopy. The samples were prepared by *in situ* cleaving to obtain a fresh surface parallel to the *bc* plane, as shown in Fig. 1(a). ARPES measurements were performed at Hiroshima
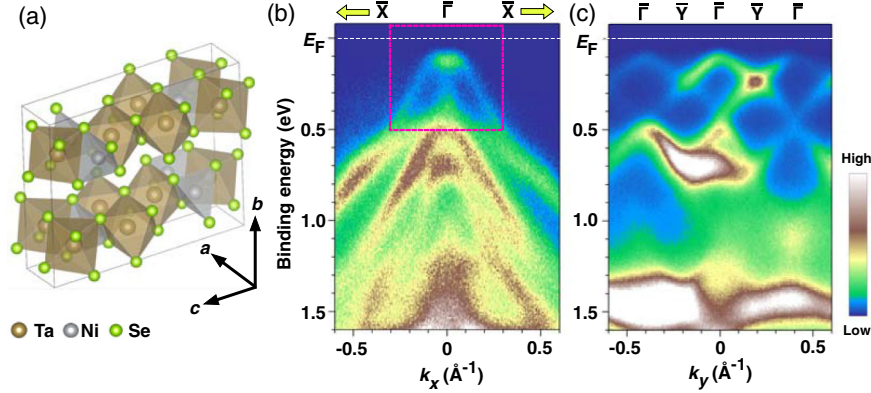
FIG. 1. (a) The unit cell of TNS crystal structure, composed of $TaSe_6$ octahedron (shaded brown) and $NiSe_4$ tetrahedron (shaded silver) each forming the chains along the a axis. (b) and (c) show the ARPES intensity plots obtained along the $\bar{\Gamma}-\bar{X}$ line [corresponds to the direction along the a axis in (a)] and $\bar{\Gamma}-\bar{Y}$ line [corresponds to the direction along the c axis in (a)], respectively. The data were obtained at $T = 40$ K and $h\nu = 30$ eV. The region surrounded by the dotted rectangle in (b) corresponds to the region shown in Fig. 2.

Synchrotron Radiation Center (HiSOR) BL-1 [29] and Pohang Light Source BL-4A2. The photon energy was set to $h\nu = 30$ eV for measurements of valence bands near the Fermi level (E_F) and $h\nu = 60$ eV for core level measurements. The temperatures of the measurements were set to $T = 40$–60 K. The K adsorption was performed at $T = 300$ K and the coverages were estimated by using a quartz microbalance and confirmed by core level intensity analyses.

Experimental results and discussion.—Figures 1(b) and 1(c) show the electronic band dispersions of TNS as revealed by the ARPES band mapping along the $\bar{\Gamma}-\bar{X}$ [along the a axis in Fig. 1(a)] and the $\bar{\Gamma}-\bar{Y}$ high symmetry directions [along the c axis], respectively. A few bands with significantly anisotropic dispersions, which are consistent with the quasi-one-dimensional crystal structure of TNS, are clearly resolved. These bands originate from the valance states of mainly Ni 3d character [12]. The close-up of the band dispersions in the vicinity of the E_F in Fig. 2(a) and the corresponding second derivative plot in Fig. 2(d) clearly

exhibit the characteristic flattening of the valence band top observed at the binding energy of $\sim$120 meV. This is in close agreement with the earlier ARPES studies [4–6], where the flattening is understood to originate from the many-body interaction in opening the band gap of the EI phase [11–13]. We have also measured a sample with a different doping level, which exhibits the flattened valence band at a different binding energy of $\sim$180 meV [Figs. 2(g) and 2(i)]. Interestingly, despite the different doping levels reflected in the $\sim$60 meV difference of the valence band energy, the shapes of the valence band top are nearly identical. This point will be discussed further below.

Upon the adsorption of K atoms, there is a discernable change in the flattop valence band as shown in Figs. 2(a)–2(f). At the K coverage of $\sim$0.035 ML, the valence band top is no longer flat, but noticeably deformed downwards near the $\bar{\Gamma}$ point [Figs. 2(b) and 2(e)]. The dip observed at the $\bar{\Gamma}$ point becomes slightly deeper upon increased K coverage of $\sim$0.07 ML [Figs. 2(c) and 2(f)], accompanied
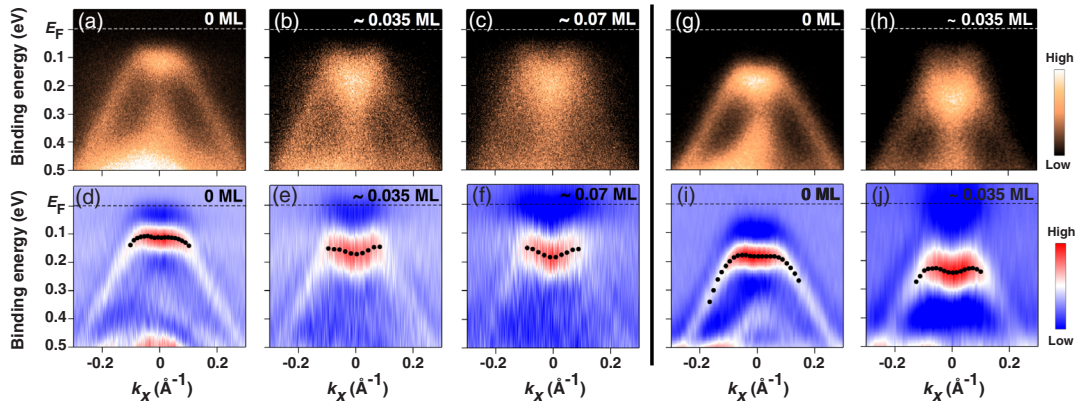
FIG. 2. The intensity plots and the corresponding second derivative plots for K/TNS as a function of K coverage, obtained for two samples with different initial doping levels. The data points overlaid for (d)–(f), (i), and (j) indicate the estimated peak positions extracted from peak fitting in the energy distribution curves (shown in Fig. S2 in Supplemental Material [30]) for various k_x.
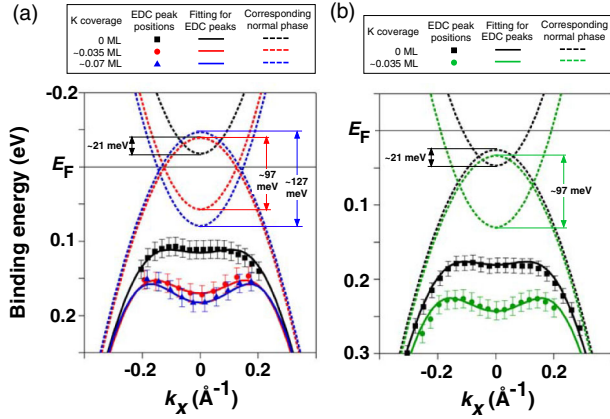
FIG. 3. The results of the band dispersion fittings for the two differently doped TNS samples, where the valence band tops are located at the binding energy of (a) ~120 meV and (b) ~180 meV. The energy distribution curve (EDC) peak positions estimated from the ARPES band mapping are shown by squares (K coverage of 0 ML), circles (~0.035 ML), and triangles (~0.07 ML). The resultant fittings to the valence bands are shown by the solid curves, while the corresponding valence and conduction bands in the normal (nonexcitonic) phase are shown by the dotted curves in respective colors indicated in the legends.

by the energy broadening of the band. The ARPES spectra taken at a much higher coverage of ~0.2 ML (Fig. S4 in the Supplemental Material [30]) solidly confirms this trend. The details of the band curvature at the valence band top is shown in Fig. 3. Figures 2(g)–2(j) show the evolution of the band dispersion upon K adsorption at ~0.035 ML for the sample with a higher initial n-doping level. Despite the difference in the initial energy of the valence band top [the binding energies of ~120 and ~180 meV, respectively, in Figs. 2(a) and 2(g)], the evolution of the valence band dispersion is consistent.

As the origin of the observed deformation in the valence band, we note two major effects expected from the K adsorption. One is the change in the carrier density, which comes from a direct electron doping from adsorbates, and the other is the electric field induced near the surface due the dipole layer formed by ionized adsorbates. The carrier density in excitonic insulators is an important factor determining the screening strength of the electron-hole attractive potential, which subsequently modifies the exciton binding energy. This effect, however, seems to be not significant in the present case. If we compare the ARPES results for the 0.07 ML K-covered TNS [Figs. 2(c) and 2(f)] and the clean TNS at a higher electron doping level [Figs. 2(g) and 2(i)], where the valence band tops are located nearly at the same energy indicating the same carrier density, we find that only the K-covered surface exhibits the valence band deformation. In addition, as mentioned above, the shape of the valence band dispersion is not affected by different doping levels of samples. These demonstrate unambiguously that

the presence of K adatoms, not merely the electron doping (the change in carrier density) is important for the observed k-dependent valence band deformation.

We then can focus on the second effect, that of the surface dipole layer. The ionized K adatoms at the surface would definitely form a dipole layer and induce an electric field perpendicular to atomic layers [along the b axis in Fig. 1(a)]. Such an electric field near the surface has been shown to cause Stark shifts of valence and conduction bands and reduce band gaps in semiconducting low-dimensional compounds [32–35] including transition metal dichalcogenides [36] and black phosphorus [37]. All these observations are simple Stark shifts for the single-particle band gap while we have to discuss the Stark effect on the many-body gap function of excitonic condensates. In order to investigate such an effect, we perform model calculations and fit the observed band dispersions using a well-established theoretical model based on a tight-binding scheme and a mean-field theory [6,20].

We take only a single pair of parabolic valence and conduction bands, whose band velocities and the single-particle band gap are set to reproduce the experimental band dispersion for the pristine sample. Note that the position of the chemical potential E_F, which does not affect band dispersions, was set to match the band positions in ARPES spectra. This overall band shape was then thought to be rigid as observed in other examples of Stark shifts, which is a good approximation for small k compared to the Brillouin zone dimension [36,37]. Then, the only fitting parameters in the model are the band gap of the non-interacting state and the excitonic order parameter Δ (corresponding to a half of the excitonic band gap). Since it was recently shown that the noninteracting band structure of TNS is a band-overlap semimetal [20,38], the band gap in the noninteracting state was a fitting parameter restricted to a negative value. There can also be an overall shift of the bands due to the electron doping. We experimentally determine such a shift by measuring Ta $4f$ core levels for the pristine and the K-adsorbed sample as shown in Fig. 4. The measured shift is 40 meV for the 0.035 ML coverage. A comparison of the model calculation and the measured band dispersions is shown in Fig. 3 for the two samples with different doping levels. The model band dispersions in the EI phase (black solid curves) exhibit excellent fits to the observed ones for the clean TNS at both doping levels with the optimized order parameter of $\Delta \sim$ 144 meV and the initial band overlap of ~22 meV. These values are fully consistent with the earlier reports [6,20]. For the K-covered TNS, the good fits to the observed band dispersions are obtained for larger band overlaps of ~97 meV (at 0.035 ML) and ~127 meV (at 0.07 ML) and an order parameter of $\Delta \sim$ 154 meV (at both 0.035 and 0.07 ML), as also shown in Fig. 3.

The deformation of the valence band top is also consistent with the dependence of the Stark shift on the orbital
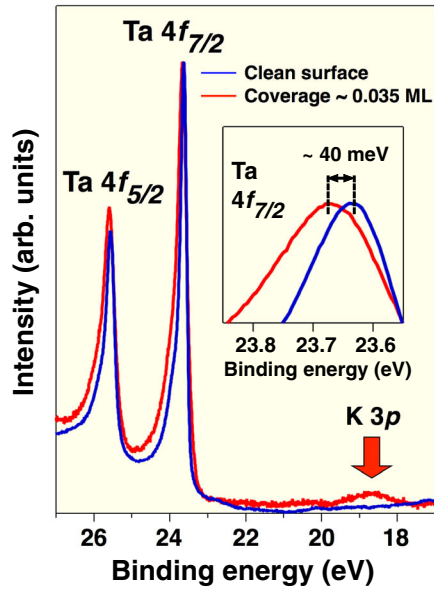
FIG. 4. The Ta $4f$ core level spectrum from clean TNS sample (blue) and from the K-covered TNS at ~0.035 ML (red). The latter also exhibits the K $3p$ core level as a small bump at the binding energy of ~18.7 eV. The inset shows the close-up of the region near the Ta $4f_{7/2}$ peak, which shows the K-induced shift of ~40 meV towards the higher binding energy.

character of the bands. At the $\bar{\Gamma}$ point in Ta_2NiSe_5, the valence band (mainly Ni $3d$ orbitals) and conduction band (mainly Ta $5d$) are strongly hybridized with each other in the EI phase [20]. Such a strong hybridization results in a rapid variation of the orbital character in momentum across $\bar{\Gamma}$, and hence the different magnitude of band shifts at different points in the valence band in the narrow vicinity of $\bar{\Gamma}$. Thus, while the overall valence band shifts upward due to the Stark effect, the top of the valence band (strongly mixed with the conduction band) around $\bar{\Gamma}$ can shift in a distinct way.

These results clearly indicate that the K adsorption on TNS causes the enhanced overlap between the valence and the conduction bands via the Stark shift, which in turn results in the observed deformations of the valence band top in the EI phase. Note that the substantial increase of the band overlap of about 70–100 meV at the K coverage below 0.1 ML is comparable to the values, a band gap narrowing of ~100 meV from 0.06–0.1 ML, observed for black phosphorus [37]. Here, it is worthwhile to note the sharp contrast between the band modifications in black phosphorus and Ta_2NiSe_5. While for the black phosphorus, the Stark shifts simply result in the crossing of the noninteracting valence and conduction bands, the Ta_2NiSe_5 exhibits the deformation of the valence bands due to the EI-induced band hybridization, which is a hallmark of a strong interaction.

From the overall rigid band shift of ~40 meV observed, the K coverage, and the dielectric constant of TNS, the

magnitude of electric field near the surface can be roughly estimated as ~60 V/μm at 0.035 ML within the simplified band-bending picture (see the Supplemental Material [30]). These values are also comparable to the corresponding values for the noticeable Stark shift in WS_2 (~170 V/μm for a ~400 meV shift) [36]. This makes it more plausible that the electric-field-induced single-particle gap reduction (i.e., the increased band overlap) leads to the deformation of the valence band top.

Interestingly, our fitting results also indicate the slight increase in the order parameter by ~10 meV upon the K adsorption (see the Supplemental Material [30] for details). This small effect might be attributed to the excitonic Stark effect [39–41]; the exciton energy level is shifted in the presence of the electric field, which enhances the binding energy of excitons. Similar effects were observed in other low-dimensional materials such as MoS_2 (~10 meV) [42] and carbon nanotubes (~3 meV) [43].

In conclusion, our investigation utilizing high-resolution ARPES on K-covered Ta_2NiSe_5 reveals that the K adsorbates cause a k-dependent deformation of the flattop valence band of the excitonic insulator phase, indicating the modification of the excitonic many-body gap function. The analyses based on a simple mean field model indicate that the main origin of this modification is the reduction of the single-particle gap (the increased overlap of the valence and conduction bands) of the normal phase by the Stark shift due to the electric field from the ionized adsorbate layer. The change in the screening effect arising from the K-induced electron doping and the excitonic Stark effect are shown to be marginal. We emphasize that the present study not only shows the fundamental behavior of the excitonic insulator in electric field, but also an important implication for the electrical manipulation of EI properties by the use of an external electric field in heterostructure-based devices.

*Corresponding author.
kfukutani@ibs.re.kr
†Corresponding author.
yeom@postech.ac.kr

[1] A. Kogar, M. S. Rak, S. Vig, A. A. Husain, F. Flicker, Y. Il Joe, L. Venema, G. J. MacDougall, T. C. Chiang,

E. Fradkin, J. van Wezel, and P. Abbamonte, Science **358**, 1314 (2017).

[2] H. Cercellier, C. Monney, F. Clerc, C. Battaglia, L. Despont, M. G. Garnier, H. Beck, P. Aebi, L. Patthey, H. Berger, and L. Forró, Phys. Rev. Lett. **99**, 146403 (2007).

[3] K. Sugawara, Y. Nakata, R. Shimizu, P. Han, T. Hitosugi, T. Sato, and T. Takahashi, ACS Nano **10**, 1341 (2016).

[4] Y. Wakisaka, T. Sudayama, K. Takubo, T. Mizokawa, M. Arita, H. Namatame, M. Taniguchi, N. Katayama, M. Nohara, and H. Takagi, Phys. Rev. Lett. **103**, 026402 (2009).

[5] Y. Wakisaka, T. Sudayama, K. Takubo, T. Mizokawa, N. L. Saini, M. Arita, H. Namatame, M. Taniguchi, N. Katayama, M. Nohara, and H. Takagi, J. Supercond. Novel Magn. **25**, 1231 (2012).

[6] K. Seki, Y. Wakisaka, T. Kaneko, T. Toriyama, T. Konishi, T. Sudayama, N. L. Saini, M. Arita, H. Namatame, M. Taniguchi, N. Katayama, M. Nohara, H. Takagi, T. Mizokawa, and Y. Ohta, Phys. Rev. B **90**, 155116 (2014).

[7] D. Jerome, T. M. Rice, and W. Kohn, Phys. Rev. **158**, 462 (1967).

[8] W. Kohn, Phys. Rev. Lett. **19**, 439 (1967).

[9] J. M. Blatt, K. W. Böer, and W. Brandt, Phys. Rev. **126**, 1691 (1962).

[10] F. J. Di Salvo, C. H. Chen, and R. M. Fleming, J. Less-Common Met. **116**, 51 (1986).

[11] T. Mizokawa, K. Takubo, T. Sudayama, Y. Wakisaka, N. Takubo, K. Miyano, N. Matsumoto, S. Nagata, T. Katayama, M. Nohara, H. Takagi, M. Ikeda, N. Kojima, M. Arita, H. Namatame, and M. Taniguchi, J. Supercond. Novel Magn. **22**, 67 (2009).

[12] T. Kaneko, T. Toriyama, T. Konishi, and Y. Ohta, Phys. Rev. B **87**, 035121 (2013).

[13] S. Ejima, T. Kaneko, Y. Ohta, and H. Fehske, Phys. Rev. Lett. **112**, 026401 (2014).

[14] T. Kaneko, T. Toriyama, T. Konishi, and Y. Ohta, J. Phys. Conf. Ser. **400**, 032035 (2012).

[15] T. I. Larkin, A. N. Yaresko, D. Pröpper, K. A. Kikoin, Y. F. Lu, T. Takayama, Y. L. Mathis, A. W. Rost, H. Takagi, B. Keimer, and A. V. Boris, Phys. Rev. B **95**, 195144 (2017).

[16] T. I. Larkin, R. D. Dawson, M. Höppner, T. Takayama, M. Isobe, Y. L. Mathis, H. Takagi, B. Keimer, and A. V. Boris, Phys. Rev. B **98**, 125113 (2018).

[17] A. Nakano, T. Hasegawa, S. Tamura, N. Katayama, S. Tsutsui, and H. Sawa, Phys. Rev. B **98**, 045139 (2018).

[18] D. Werdehausen, T. Takayama, M. Höppner, G. Albrecht, A. W. Rost, Y. Lu, D. Manske, H. Takagi, and S. Kaiser, Sci. Adv. **4**, eaap8652 (2018).

[19] S. Y. Kim, Y. Kim, C.-J. Kang, E.-S. An, H. K. Kim, M. J. Eom, M. Lee, C. Park, T.-H. Kim, H. C. Choi, B. I. Min, and J. S. Kim, ACS Nano **10**, 8888 (2016).

[20] J. Lee, C.-J. Kang, M. J. Eom, J. S. Kim, B. I. Min, and H. W. Yeom, Phys. Rev. B **99**, 075408 (2019).

[21] Y. F. Lu, H. Kono, T. I. Larkin, A. W. Rost, T. Takayama, A. V. Boris, B. Keimer, and H. Takagi, Nat. Commun. **8**, 14408 (2017).

[22] S. Mor, M. Herzog, D. Golež, P. Werner, M. Eckstein, N. Katayama, M. Nohara, H. Takagi, T. Mizokawa, C. Monney, and J. Stähler, Phys. Rev. Lett. **119**, 086401 (2017).

[23] Y. Murakami, D. Golež, M. Eckstein, and P. Werner, Phys. Rev. Lett. **119**, 247601 (2017).

[24] J. I. A. Li, T. Taniguchi, K. Watanabe, J. Hone, and C. R. Dean, Nat. Phys. **13**, 751 (2017).

[25] X. Liu, K. Watanabe, T. Taniguchi, B. I. Halperin, and P. Kim, Nat. Phys. **13**, 746 (2017).

[26] A. A. Zibrov, C. Kometter, H. Zhou, E. M. Spanton, T. Taniguchi, K. Watanabe, M. P. Zaletel, and A. F. Young, Nature (London) **549**, 360 (2017).

[27] L. Du, X. Li, W. Lou, G. Sullivan, K. Chang, J. Kono, and R.-R. Du, Nat. Commun. **8**, 1971 (2017).

[28] W. Yu, V. Clericò, C. H. Fuentevilla, X. Shi, Y. Jiang, D. Saha, W. K. Lou, K. Chang, D. H. Huang, G. Gumbs, D. Smirnov, C. J. Stanton, Z. Jiang, V. Bellani, Y. Meziani, E. Diez, W. Pan, S. D. Hawkins, and J. F. Klem, New J. Phys. **20**, 053062 (2018).

[29] H. Iwasawa, K. Shimada, E. F. Schwier, M. Zheng, Y. Kojima, H. Hayashi, J. Jiang, M. Higashiguchi, Y. Aiura, H. Namatame, and M. Taniguchi, J. Synchrotron Radiat. **24**, 836 (2017).

[30] See Supplemental Material at http://link.aps.org/supplemental/10.1103/PhysRevLett.123.206401 for computational methods and additional data, which includes Refs. [6,15,31].

[31] A. F. Santander-Syro, O. Copie, T. Kondo, F. Fortuna, S. Pailhès, R. Weht, X. G. Qiu, F. Bertran, A. Nicolaou, A. Taleb-Ibrahimi, P. Le Fèvre, G. Herranz, M. Bibes, N. Reyren, Y. Apertet, P. Lecoeur, A. Barthélémy, and M. J. Rozenberg, Nature (London) **469**, 189 (2011).

[32] K. H. Khoo, M. S. C. Mazzoni, and S. G. Louie, Phys. Rev. B **69**, 201401(R) (2004).

[33] M. Ishigami, J. D. Sau, S. Aloni, M. L. Cohen, and A. Zettl, Phys. Rev. Lett. **94**, 056804 (2005).

[34] A. Ramasubramaniam, D. Naveh, and E. Towe, Phys. Rev. B **84**, 205325 (2011).

[35] N. Zibouche, P. Philipsen, A. Kuc, and T. Heine, Phys. Rev. B **90**, 125440 (2014).

[36] M. Kang, B. Kim, S. H. Ryu, S. W. Jung, J. Kim, L. Moreschini, C. Jozwiak, E. Rotenberg, A. Bostwick, and K. S. Kim, Nano Lett. **17**, 1610 (2017).

[37] J. Kim, S. S. Baik, S. H. Ryu, Y. Sohn, S. Park, B. G. Park, and K. S. Kim, Science **349**, 723 (2015).

[38] K. Sugimoto, S. Nishimoto, T. Kaneko, and Y. Ohta, Phys. Rev. Lett. **120**, 247602 (2018).

[39] A. E. Cherednichenko and V. A. Kiselev, Prog. Surf. Sci. **36**, 179 (1991).

[40] D. F. Blossey, Phys. Rev. B **2**, 3976 (1970).

[41] D. F. Blossey, Phys. Rev. B **3**, 1382 (1971).

[42] M. Yoshida, Y. Kumamoto, A. Ishii, A. Yokoyama, and Y. K. Kato, Appl. Phys. Lett. **105**, 161104 (2014).

[43] J. Klein, J. Wierzbowski, A. Regler, J. Becker, H. Heimbach, K. Muller, M. Kaniber, and J. J. Finley, Nano Lett. **16**, 1554 (2016).